

Hall effect and thermoelectric power in UNiGa

Y. Kobayashi,* Y. Aoki, H. Sugawara, and H. Sato

Department of Physics, Tokyo Metropolitan University, Hachioji-shi, Tokyo 192-03, Japan

V. Sechovsky and L. Havela

Department of Metal Physics, Charles University, CZ-12 116 Prague 2, The Czech Republic

K. Prokes, M. Mihalik, and A. Menovsky

Van der Waals-Zeeman Institute, University of Amsterdam, NL-1018 XE Amsterdam, The Netherlands

(Received 8 July 1996)

We report on simultaneous measurements of the magnetization, magnetoresistance, Hall effect and thermoelectric power on single-crystal UNiGa to investigate the origin of giant magnetoresistance phenomena. The normal part of Hall coefficient is markedly different above and below the metamagnetic transition at low temperatures. The thermoelectric power at 4.2 K changes its sign between the two magnetic states. These results imply that the strong resistivity variations are intimately connected with a reconstruction of the Fermi surface across the transition. [S0163-1829(96)07346-8]

The uranium intermetallic compound UNiGa crystallizes in the hexagonal structure of the ZrNiAl type. It undergoes a sequence of magnetic phase transitions in the temperature range 35–39.5 K. The ground state antiferromagnetic (AF) structure is characterized by the *c*-axis stacking (+ + - + - -) of U moments ferromagnetically ordered within basal plane sheets.^{1,2} A strong uniaxial anisotropy keeps the moments aligned along the *c* axis in all magnetic structures. As shown in the magnetic phase diagram (see Fig. 1), the magnetic field applied along the *c* axis induces a metamagnetic transition leading to a ferromagnetic (F) stacking.² This transition, which is of the first-order type with considerable hysteresis is at $T=4.2$ K and at $B_c \sim 0.8$ T, splits into two steps for $T > 15$ K. In the intermediate fields the structure of the (+ + -) type was detected. The size of U moments ($1.3 \mu_B/\text{f.u.}$ at $T=4.2$ K) is practically independent of the type of the structure. One of the most prominent features of UNiGa is the reduction of electrical resistivity in the metamagnetic state. Especially, the resistivity for current along the *c* axis, which is most affected by variations of the U moments stacking, drops nearly by one order of magnitude.^{2,3} Two mechanisms are usually considered as origins of such giant magnetoresistance (GMR) effect.⁴ One possible mechanism is a spin-dependent scattering mechanism leading to a reduction of the relaxation time in the AF state, which is commonly considered in magnetic multilayer systems.⁵ However, it may not be reasonable to assume the scattering due to the disorder at interlayer boundaries and the spin-split density of states for each U monolayer. Another possibility is the variations of the Fermi surface when crossing the metamagnetic transition (for example, due to the disappearance of the superzone gap resulting from the F ordering), which yield the variation of the electronic specific heat coefficient γ . Recently, specific-heat measurements extended to very low temperatures showed that the γ value, which is 48 (mJ/mol K²) in the high field F state, decreases by about 10% in the AF state.⁶

To make clear the origin of the GMR in UNiGa, measurements of the transport properties such as Hall effect and thermoelectric power are desirable. The Hall resistivity in magnetic materials is described as a sum of two terms; the normal Hall resistivity and the extraordinary one. The normal Hall effect contains information on Fermi surface such as carrier concentration and/or the **k** dependence of the conduction electron scattering.⁷ The extraordinary Hall effect provides information on the left-right asymmetry of the scattering.⁷ The thermoelectric power contains terms of the energy derivative of the density of states and that of relax-

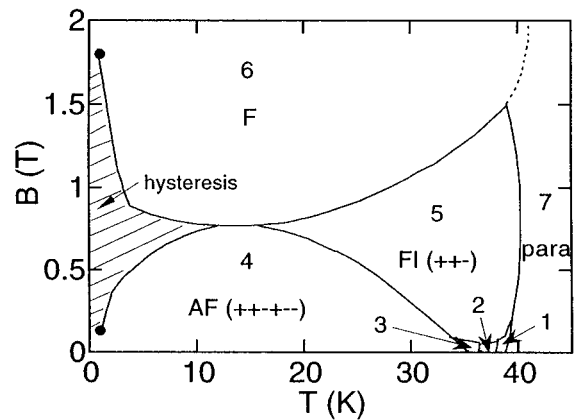


FIG. 1. Magnetic phase diagram of UNiGa for magnetic fields applied along the *c* axis. The full circles at $T=1$ K was determined from the specific heat measurement in Ref. 6. (1) incommensurate AF structure, $q = \pm(0,0,\delta)$, $\delta \sim 0.36$; (2) AF phase with $q = \pm(0,0,1/3)$, e.g., the structure with frustrated “paramagnetic” moments in each third U-T plane, i.e., (+0-); (3) AF phase with the (+ + - + - -) stacking, $q = \pm(0,0,1/8)$, $\pm(0,0,3/8)$; (4) AF phase with the (+ + - + - -) stacking, $q = \pm(0,0,1/2)$, $\pm(0,0,1/3)$, $\pm(0,0,1/6)$; (5) uncompensated AF (ferrimagnetic) phase with the (+ + -) stacking, $q = \pm(0,0,1/3)$; (6) ferromagnetic phase, $q = \pm(0,0,0)$; (7) paramagnetic phase.

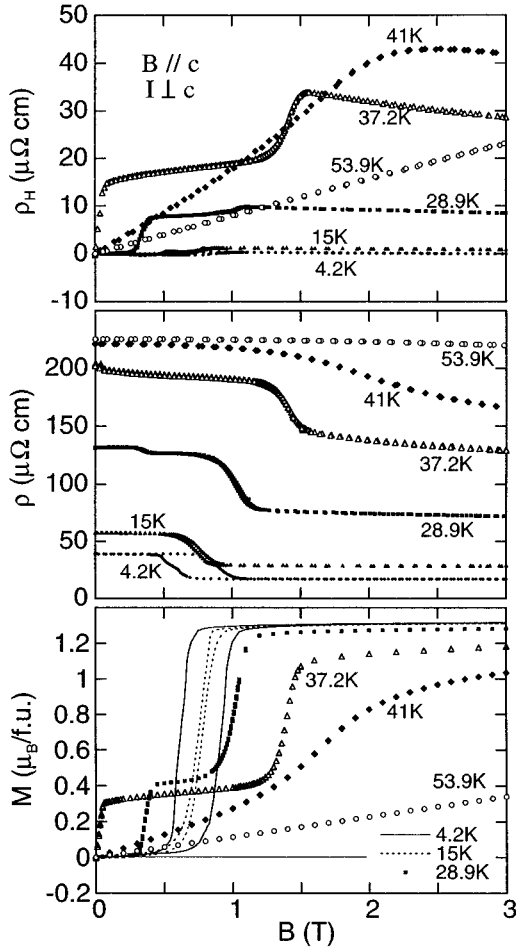


FIG. 2. Field dependence of the resistivity (ρ), Hall resistivity (ρ_H), and magnetization (M) for magnetic field $B \parallel c$ and current $I \perp c$ at selected temperatures.

ation time of the conduction electrons.⁸

In this paper, we report on simultaneous measurement of the resistivity, Hall effect, thermoelectric power, and magnetization on a UNiGa single crystal.

The single crystal of UNiGa has been grown from a stoichiometric melt in triarc Czochralski equipment. Bar shaped samples (typically $4 \times 1 \times 0.5$ mm) were cut to measure transport properties for current I (temperature gradient ΔT) perpendicular to the c axis. The Hall effect and resistivity were measured by a conventional dc four-probe method using a computer controlled current source and KEITHLEY 182 nanovoltmeters. The thermoelectric power was measured by a differential method using AuFe-chromel differential thermocouples. Magnetic field was applied using a superconducting magnet with field up to 5 T and an iron-core electromagnet up to 1.5 T. Magnetization measurements were performed on a SQUID magnetometer.

Figure 2 shows the field dependence of the electrical resistivity (ρ), Hall resistivity (ρ_H) and magnetization (M) for magnetic field $B \parallel c$ axis and $I \perp c$ at selected temperatures. The Hall resistivity $\rho_H(B)$ shows a steplike increment with increasing field at the metamagnetic transitions. In the intermediate temperature range (seen well for $T=28.9$ K) one can see double steps, the first of them being due to the transition to the $(++-)$ phase. The increase is noticeable especially

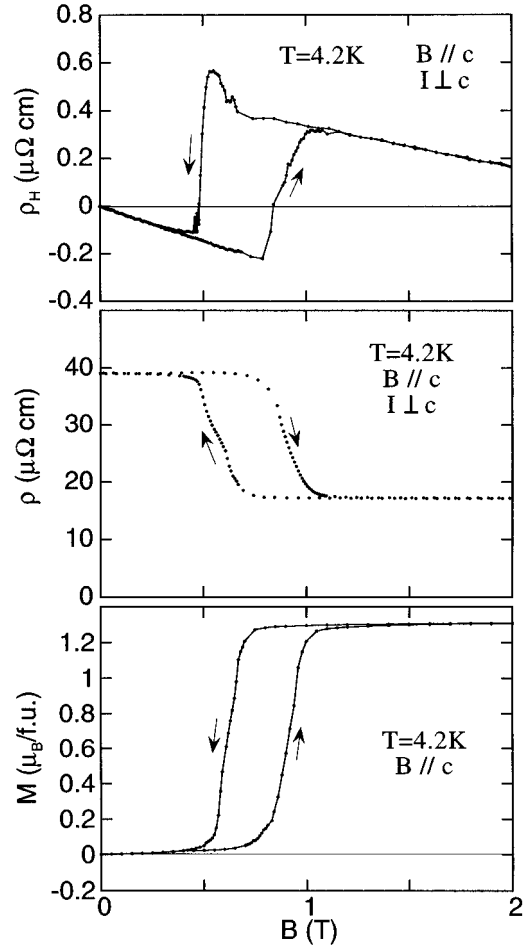


FIG. 3. Detail of the Fig. 2 at $T=4.2$ K.

near the ordering temperature, which manifests the contribution of the extraordinary Hall effect resulting from the magnetic scattering. At low temperatures, the absolute value of the change of ρ_H is much smaller. In ordinary ferromagnetic materials, $\rho_H(B)$ is described empirically as a sum of two terms; the normal Hall resistivity and the extraordinary one:

$$\rho_H(B) = R_H B = R_0 B + R_S M, \quad (1)$$

where R_0 and R_S are the normal and the extraordinary Hall coefficient, respectively, and M is the volume magnetization.⁷ In ordinary ferromagnetic materials, the determination of the field dependence of the two contributions is possible only for higher fields where the magnetization M saturates. However, for UNiGa at low temperatures (see Fig. 3), we can derive the normal part of ρ_H for the fields both above and below B_c , where both ρ and M depends only weakly on magnetic field in the two regions, which makes the extraordinary part of the Hall resistivity (ρ_H^M) to be almost constant. In fact, at $T=4.2$ K, the field dependence of $\rho_H(B)$ is almost linear in the fields below and above B_c as shown in Fig. 3, which suggests that the normal Hall effect predominates in the slope of the $\rho_H(B)$ in both regions. The most significant result shown in Fig. 3 is the difference in the slope between the AF region below B_c and F region above B_c . The value of R_0 estimated from the slope of $\rho_H(B)$ is -2.9 ± 0.1 (10^{-9} m³/C) for the AF state and -1.7 ± 0.1 (10^{-9}

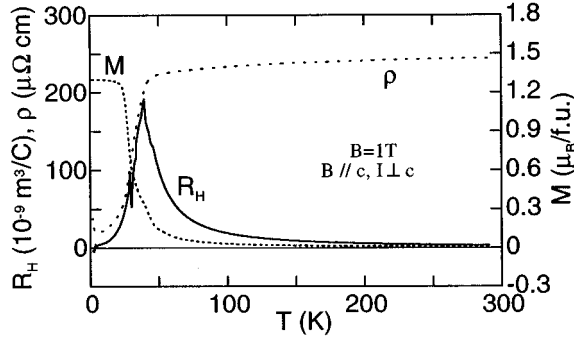


FIG. 4. Temperature dependence of Hall coefficient (R_H), ρ and M at $B=1$ T.

m^3/C) for the F state. We found no essential change of these values down to $T=2$ K. The difference in R_0 in the two phases evidences a considerable change of the Fermi surface resulting from the spin reorientation, which takes part in the GMR effect.

The anomaly manifested in $\rho_H(B)$ as a peak at $B \sim 0.5$ T for decreasing field. An anomaly can be seen also in $\rho(B)$ and $M(B)$ curves around $B \sim 0.5$ T. In a previous study, an anomaly in $M(B)$ indicates a tendency to form another phase with $M=1/3M_s$ for decreasing field. According to these facts, we infer that the peak in $\rho_H(B)$ is yielded by the increase of the left-right asymmetric scattering due to the partial increment of the spin-randomness accompanied by the spin reorientation.

To investigate the characteristics of magnetic scattering, we analyze the extraordinary part of Hall effect. Figure 4 shows the temperature dependence of the Hall coefficient (R_H), ρ and M at $B=1$ T. Such field induces the ferromagnetic alignment at temperatures below about 30 K, whereas in the range 30–40 K it leads to the uncompensated AF phase ($++-$). Both phase transitions are reflected in all the quantities shown.

In the paramagnetic state, R_H increases with decreasing temperature resembling the $M(T)$ dependence, suggesting the predominance of the extraordinary Hall effect. The origin of the left-right asymmetric scattering responsible for the extraordinary Hall effect can be classified into two mechanisms; the skew scattering proportional to ρ and the side-jump scattering proportional to ρ^2 . It is known that in paramagnetic state only the skew scattering contributes to the extraordinary Hall effect, while both mechanisms contribute in the ferromagnetic state.⁷ In general, the R_S for ferromagnetic state can be described as

$$R_S = a\rho + b\rho^2. \quad (2)$$

If only the skew scattering contributes to the extraordinary Hall effect of UNiGa in paramagnetic state, R_H is then expected to be a straight line as a function of ρM . R_H plotted against ρM is shown in Fig. 5, using the data from Fig. 4. The data are indeed approximately on a straight line above $T \sim 50$ K, confirming that the skew scattering is responsible for the extraordinary Hall effect in the paramagnetic state, as expected.⁷ From the intercept of the plot, R_0 was estimated to be -2.2 ± 0.2 ($10^{-9} \text{ m}^3/\text{C}$), which is close to the value obtained in the ferromagnetic state.

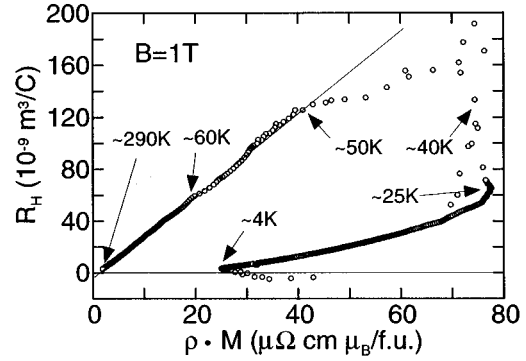


FIG. 5. R_H versus ρM plot at $B=1$ T. For details see the text.

According to Eq. (2), the R_S/ρ versus ρ plot in the ferromagnetic state should be a straight line, and the contribution of the skew and side-jump scattering mechanisms can be separated. To analyze the data in the ferromagnetic state, we plot R_S/ρ versus ρ at $B=1$ and 5 T (see Fig. 6) using the data from the Figs. 4 and 2. To obtain the values of R_S , we subtracted the respective values of the normal part R_0 for antiferromagnetic and ferromagnetic regions at $T=4.2$ K, assuming each R_0 to be independent of temperature. The R_S/ρ data in ferromagnetic state (at $B=1$ T above about 4 K up to about 30 K and at $B=5$ T up to 41 K) are almost proportional to ρ . Thus we can deduce that the side-jump scattering dominates the extraordinary Hall effect in the ferromagnetic state, as observed in ordinary ferromagnetic materials.⁷ The parameters can be estimated as $a=1.2 \pm 0.1$ (10^{-3} T^{-1}) and $b=60 \pm 1$ ($10^{-4} [\mu\Omega \text{ cm}]^{-1} \text{ T}^{-1}$), respectively. The magnitude of b is about ten times larger than ordinary ferromagnetic materials,^{9,10} showing the large side-jump scattering in UNiGa. This result suggests the contribution of the polarized $5f$ -band ferromagnetism due to the strong hybridization between $5f$ and conduction electrons in UNiGa, because a large side-jump scattering cannot be explained unless the contribution of itinerant electron ferromagnetism is taken into account.⁷ The itinerant character of $5f$ electrons can be deduced also from the size of the U moments of $1.3 \mu_B/\text{f.u.}$ which is much smaller than that expected for ionic $5f^3$ or $5f^2$ configurations.

Figure 7 shows the temperature dependence of the thermoelectric power (S) at $B=0$ and 1 T. At zero field, S is negative at higher temperatures and almost linear above 100 K. Near $T=40$ K, S changes the sign and shows double

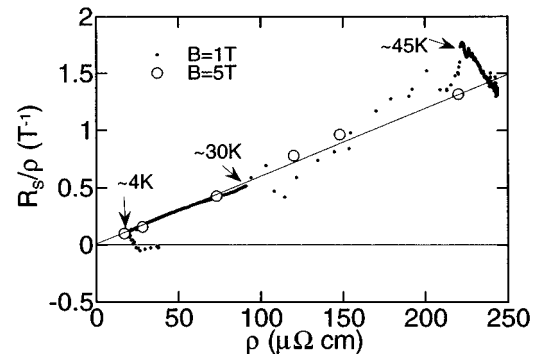


FIG. 6. $R_S(T)/\rho(T)$ versus $\rho(T)$ plot at $B=1$ and 5 T.

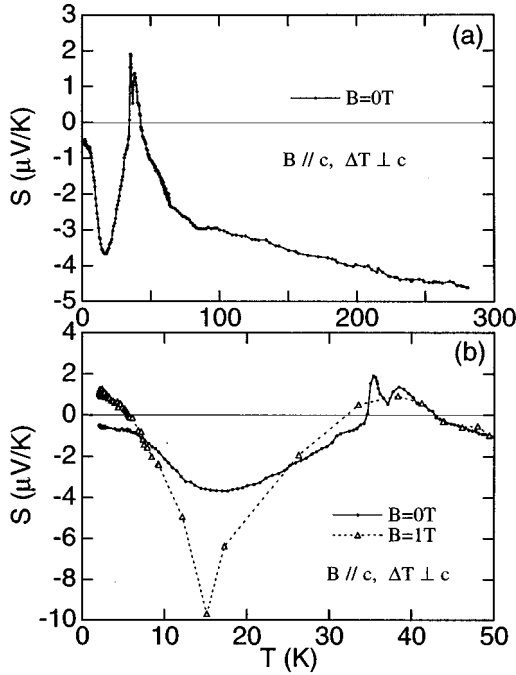


FIG. 7. (a) Temperature dependence of thermoelectric power (S) at $B=0$ T and (b) that below 50 K at $B=0$ and 1 T.

peaks, which reflects the complex phase diagram (see Fig. 1). With decreasing temperature, $S(T)$ becomes negative again below $T \sim 35$ K showing a minimum around 15 K. At $B=1$ T, $S(T)$ at higher temperatures is almost identical to that at zero field. On the other hand, the thermoelectric power characteristics at low temperatures are largely different; the absolute values around the minimum become much larger and the sign of S changes again from negative to positive below $T=6$ K. The sign change of S between $B=0$ and 1 T were confirmed by measurements of the field dependence of S at $T=4.2$ K, as shown in Fig. 8. According to the Mott equation for thermoelectric power, we can write

$$S = -\frac{\pi^2 k_B^2}{3|e|} T \left[\frac{\partial \ln N(E)}{\partial E} + \frac{\partial \ln \tau(E)}{\partial E} \right]_{E=E_F}, \quad (3)$$

where $N(E)$ is the density of states and $\tau(E)$ is the relaxation time of conduction electrons.⁸ Thus the sign change of S at $T=4.2$ K might reflect the sign change of the energy derivative of the density of states at the Fermi level due to the Fermi surface reconstruction connected with the transition. However, at $T=15$ K, the absolute value of S increases without sign change (see Fig. 8), suggesting the existence of another temperature dependent contribution to S such as the contribution of the energy dependence of the scattering rate. The Fermi surface change cannot solely explain the difference of S between $B=0$ and 1 T around $T=15$ K.

The strong variations both in the Hall effect and thermoelectric power with the reorientation of U-magnetic moments point to an importance of the Fermi surface change of UNiGa at the metamagnetic transition, suggesting the superzone gap formation. As the Fermi surface can be intersected by the new Brillouin zone boundaries, which leads generally

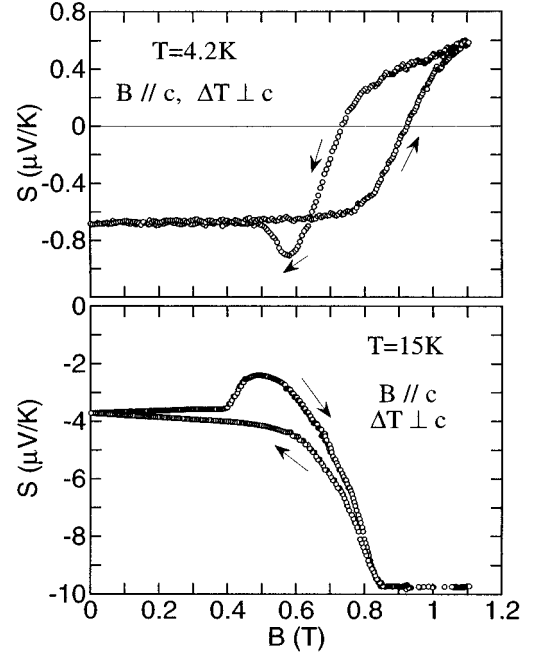


FIG. 8. Field dependence of the S at $T=4.2$ and 15 K.

to gapping in electron dispersion relations, the density of states at the Fermi level can be substantially reduced in the AF state, which leads to the decrease of the γ coefficient and the reduction of carrier concentration and consequently to the increase of ρ .¹¹ This interpretation is qualitatively supported by the recent specific heat measurements, which show higher γ value in the F state.⁶ However, the variation of γ value is only 10%, which is not enough to explain the strong variation of the ρ if the γ value reflects only the carrier concentration. We should take account of another mechanism to explain the GMR. One possible origin is the Fermi velocity change resulting from the change of the band structure between AF and F phases, which has been discussed by Oguchi to explain the GMR for magnetic multilayers.¹² Some of the band branches which cross the Fermi energy near the AF zone boundaries show a smaller gradient of the energy bands in the AF phase, leading a smaller Fermi velocity. Therefore, the large resistivity is expected for AF state. To clarify the Fermi velocity effect, further investigation such as the band structure calculation is desirable.

In conclusion, we found a striking difference in the normal Hall effect coefficient R_0 between antiferromagnetic and ferromagnetic phases at low temperatures. The thermoelectric power changes even its sign across the metamagnetic transition. These facts bring convincing evidences of the Fermi surface reconstruction due to the transition from antiferromagnetic phase to ferromagnetic one, which can contribute to the giant magnetoresistance effect. In the field-induced ferromagnetic state, the side-jump scattering dominates the extraordinary part of the Hall resistivity, which corroborates the itinerant character of $5f$ electrons.

This work was supported by a Grant-in-Aid for Scientific Research from the Ministry of Education, Science and Culture of Japan and by the Czech Grant Agency under Grant No. 202/96/0207.

*Electronic address: koba@phys.metro-u.ac.jp

¹V. Sechovsky, L. Havela, E. Brück, F. R. de Boer, and A. V. Andreev, *Physica B* **163**, 103 (1990).

²K. Prokes, E. Brück, F. R. de Boer, M. Mihalik, A. Menovsky, P. Burllet, J. M. Mignot, L. Havela, and V. Sechovsky, *J. Appl. Phys.* **79**, 6396 (1996).

³V. Sechovsky, L. Havela, L. Jirman, W. Ye, T. Takabatake, H. Fujii, E. Brück, F. R. de Boer, and H. Nakotte, *J. Appl. Phys.* **70**, 5794 (1991).

⁴L. Havela, V. Sechovsky, K. Prokes, H. Nakotte, H. Fujii, and A. Lacerda, *Physica B* **223&224**, 245 (1996).

⁵H. Sato, H. Henmi, Y. Kobayashi, Y. Aoki, H. Yamamoto, T. Shinjo, and V. Sechovsky, *J. Appl. Phys.* **76**, 6919 (1994), and references therein.

⁶Y. Aoki, Y. Kobayashi, H. Sato, H. Sugawara, V. Sechovsky, L. Havela, K. Prokes, M. Mihalik, and A. Menovsky, *J. Phys. Soc. Jpn.* **65**, 3312 (1996).

⁷L. Berger and G. Bergmann, in *The Hall Effect and Its Applications*, edited by C. L. Chien and C. R. Westgate (Plenum, New York, 1980), p. 55.

⁸R. D. Barnard, *Thermoelectricity in Metals and Alloys* (Taylor, London, 1972).

⁹G. C. Carter and E. M. Pugh, *Phys. Rev.* **152**, 498 (1963).

¹⁰R. Asomoza, A. Fert, and R. Reich, *J. Less-Common Met.* **90**, 177 (1983).

¹¹R. J. Elliot and F. A. Wedgwood, *Proc. Phys. Soc. London* **81**, 846 (1963).

¹²T. Oguchi, *Mater. Sci. Eng. B* **31**, 111 (1995).